




Quantifying irrigation uptake in olive trees: a proof-of-concept approach combining isotope tracing and Hydrus-1D

Paolo Nasta, Diego Todini-Zicavo, Giulia Zuecco, Chiara Marchina, Daniele Penna, Jeffrey J. McDonnell, Anam Amin, Carolina Allocca, Fabio Marzaioli, Luisa Stellato, Marco Borga & Nunzio Romano


To cite this article: Paolo Nasta, Diego Todini-Zicavo, Giulia Zuecco, Chiara Marchina, Daniele Penna, Jeffrey J. McDonnell, Anam Amin, Carolina Allocca, Fabio Marzaioli, Luisa Stellato, Marco Borga & Nunzio Romano (2023): Quantifying irrigation uptake in olive trees: a proof-of-concept approach combining isotope tracing and Hydrus-1D, Hydrological Sciences Journal, DOI: [10.1080/02626667.2023.2218552](https://doi.org/10.1080/02626667.2023.2218552)


To link to this article: <https://doi.org/10.1080/02626667.2023.2218552>

 [View supplementary material](#)

 Published online: 20 Jun 2023.

 [Submit your article to this journal](#)

 Article views: 66

 [View related articles](#)

 [View Crossmark data](#)



TECHNICAL NOTE

Quantifying irrigation uptake in olive trees: a proof-of-concept approach combining isotope tracing and Hydrus-1D

Paolo Nasta ^a, Diego Todini-Zicavo^{b,c}, Giulia Zuecco ^{b,d}, Chiara Marchina ^b, Daniele Penna ^e, Jeffrey J. McDonnell ^{f,g}, Anam Amin ^b, Carolina Allocca^a, Fabio Marzaioli^h, Luisa Stellato^h, Marco Borga ^b and Nunzio Romano ^a

^aDepartment of Agricultural Sciences, AFBE Division, University of Naples Federico II, Portici, Naples, Italy; ^bDepartment of Land, Environment, Agriculture and Forestry, University of Padova, Legnaro, Italy; ^cDepartment of Science Technology and Society, University School for Advanced Studies (IUSS), Pavia, Italy; ^dDepartment of Chemical Sciences, University of Padova, Padua, Italy; ^eDepartment of Agriculture, Food, Environment and Forestry (DAGRI), University of Florence, Florence, Italy; ^fGlobal Institute for Water Security and School of Environment and Sustainability, University of Saskatchewan, Saskatoon, Saskatchewan, Canada; ^gSchool of Geography, Earth & Environmental Sciences, University of Birmingham, Birmingham, UK; ^hCentre for Isotopic Research on Cultural and Environmental Heritage (CIRCE), Department of Mathematics and Physics, University of Campania “Luigi Vanvitelli”, Caserta, Italy

ABSTRACT

An isotope-enabled module of Hydrus-1D was applied to a potted olive tree to trace water parcels originating from 26 irrigation events in a glasshouse experiment. The soil hydraulic parameters were optimized via inverse modelling by minimizing the discrepancies between observed and simulated soil water content and soil water isotope (^{18}O) values at three soil depths. The model's performance was validated with observed sap flow z-scores and xylem water ^{18}O . We quantified the source and transit time of irrigation water by analysing the mass breakthrough curves derived from a virtual tracer injection experiment. On average, 26% of irrigation water was removed by plant transpiration with a mean transit time of 94 hours. Our proof of concept work suggests that transit time may represent a functional indicator for the uptake of irrigation water in agricultural ecosystems.

ARTICLE HISTORY

Received 23 August 2022
Accepted 26 April 2023

EDITOR

A. Fiori

ASSOCIATE EDITOR

(not assigned)

KEYWORDS

transit time; soil water content; sap flow; root water uptake; virtual tracer injection experiment; isotope labelling experiment

1 Introduction

Understanding how plants take up soil water originating from individual irrigation events is key to agricultural water sustainability. However, quantifying plant water use, stress, and resilience represents a major scientific challenge for improving the design of appropriate irrigation-based water management strategies (Jackisch *et al.* 2020). A key factor is the transit time of irrigation water from when it enters through the soil surface to its exit as root water uptake (RWU). This transit time is a key metric to describe the temporal origin of RWU (von Freyberg *et al.* 2020). Stable isotopes of hydrogen (^2H) and oxygen (^{18}O) represent valuable tools to estimate transit time and source water mixtures in the soil–plant–atmosphere continuum (SPAC) (e.g. Stumpp *et al.* 2012, Penna *et al.* 2018, Benettin *et al.* 2021, Beyer and Penna 2021), especially in agricultural systems (e.g. Beyer *et al.* 2018, Penna *et al.* 2020, 2021, Kahmen *et al.* 2021, Mennekes *et al.* 2021, Aguzzoni *et al.* 2022, Barbeta *et al.* 2022, Chen *et al.* 2022).

Recently, the temporal origin of RWU has been determined by tracking water parcels introduced with individual labelled rainfall or irrigation events into the soil profile (Sprenger *et al.* 2016, Asadollahi *et al.* 2022). These studies have used virtual tracer injection experiments to assess RWU dynamics under

different environmental conditions. Nevertheless, interpreting RWU dynamics and understanding the temporal origin of RWU by exploiting process-oriented hydrological models is still needed. Here we built on an isotope labelling approach in a potted olive tree experiment performed by Amin *et al.* (2021) as the basis of our model approach. We present a proof-of-concept modelling analysis that combines isotope tracing and the water flow in Hydrus-1D to explore the temporal origin of RWU. Our specific objectives are: (i) to simulate water flow and isotope transport in the potted olive tree system by optimizing the soil hydraulic parameters via inverse modelling; and (ii) to simulate the RWU transit times and the contribution of irrigation water to actual transpiration using a virtual tracer experiment based on an ensemble simulation approach.

2 Materials and methods

2.1 Experimental set-up, monitoring and sampling approach

Two 6-year-old olive trees (*Olea europaea*; 0.06 m diameter and 1.9 m height) were placed in a glasshouse at the Department of Land, Environment, Agriculture and Forestry of the University of Padova (Italy). The two olive trees (named

O1 and O2) were positioned in 70-L draining plastic pots (height of 42.0 cm) containing a soil mixture of 80% sandy loam and 20% pumice repacked at an oven-dry soil bulk density of 1.45 g cm^{-3} with a corresponding soil porosity of $0.45 \text{ cm}^3 \text{ cm}^{-3}$ (Amin *et al.* 2021). The soil in each pot was covered with a plastic film to limit the evaporation losses from the soil surface (Fig. 1). The experiment lasted seven weeks, from 16 May 2018 to 6 July 2018 for a total of 52 days (corresponding to 1234 hours considering the initial time on 16 May at midnight and the final time on 6 July at 9.00am).

Air temperature, relative air humidity, and global solar radiation were measured at five-minute intervals by a weather station installed inside the glasshouse, at a distance of 1 m from the two olive trees. Daily values of reference evapotranspiration (ET_0) were calculated using the standard physically-based Penman-Monteith equation (Allen *et al.* 1998). Crop-specific potential evapotranspiration (ET_c) under standard conditions without water limitations (the pot was frequently irrigated during the experiment) was calculated by multiplying ET_0 by the specific crop coefficient, K_c (i.e. $ET_c = ET_0 \times K_c$). The crop coefficient (K_c ; dimensionless) for the olive tree was assumed to be $K_c = 0.75$ (Rallo *et al.* 2010). The roots were distributed along the entire soil profile at the end of the experiment, therefore, the maximum root depth (z_r in cm) was assumed to be $z_r = 42 \text{ cm}$. Potential transpiration, T_p , was assumed to equal ET_c since surface evaporation was set to zero.

Thermal dissipation sensors were installed in the stems of both trees to record sap flow rates at five-minute intervals (Granier 1985). Measurements of near-surface soil water content (0–6 cm soil depth) were taken twice a day (morning and evening) using a ThetaProbe soil moisture sensor (ML2x type 2 ThetaProbe, Delta-T devices, Cambridge, UK). At the completion of the experiment, the soil capacitance readings were calibrated and converted into soil water contents through an empirical equation (Amin *et al.* 2021).

Stable isotopes of hydrogen and oxygen were used for the tracer experiment. The experiment duration was split into a 2-week conditioning period and a labelling period. The former began on 16 May 2018 when the plants were irrigated with 3 L of

local tap water ($\delta^2\text{H}$ of $-52.3\text{‰} \pm 1.8\text{‰}$ and a $\delta^{18}\text{O}$ of $-7.97\text{‰} \pm 0.77\text{‰}$) every two days; the latter followed the conditioning period, and the potted trees were irrigated with 2, 3, or 5 L of labelled water ($\delta^2\text{H}$: $-93.3\text{‰} \pm 1.8\text{‰}$, and $\delta^{18}\text{O}$: $-12.75\text{‰} \pm 0.50\text{‰}$) approximately every two days for five weeks (Amin *et al.* 2021).

Soil and twig samples for isotopic analyses were taken at the end of each week of the experiment. The twig samples were collected along the entire length of each selected branch, and the bark was removed before storing the samples. Soil cores were collected at three depths, i.e. 0–5, 5–15, and 15–25 cm. All samples were stored in airtight 12 mL Labco Exetainer® glass vials (Labco Ltd., Lampeter, UK). At the end of the experiment (6 July 2018), additional soil and plant samples were retrieved completely from O1 while the usual sampling was carried out from O2 (considered a replicate) (Amin *et al.* 2021). Irrigation water samples were collected from the tap water and labelled water for isotopic analysis. All the samples were stored in the refrigerator until the isotopic analysis.

The extraction of soil and xylem water was carried out using the cryogenic vacuum distillation (CVD) method (Koeniger *et al.* 2011), performed in two different laboratories, at the Faculty of Science and Technology, Free University of Bozen-Bolzano (Italy), and at the Global Institute for Water Security, University of Saskatchewan (Canada). A detailed description of the two CVD systems used in this work can be found in Amin *et al.* (2021). Data analysis showed that there was not a clear effect of the CVD system on the isotopic composition of the extracted soil and plant waters (Amin *et al.* 2021). Therefore, in this study, we only considered $\delta^{18}\text{O}$ data from O1 obtained from the samples extracted at the Global Institute for Water Security, University of Saskatchewan (Canada). The isotopic composition of xylem water was determined by isotope ratio mass spectrometry at InnoTech Alberta (Edmonton, Canada), whereas the isotopic compositions of irrigation and soil water were measured by a Picarro isotope analyser (cavity ring-down spectroscopy method, model L2130-i, manufactured by Picarro Inc.,

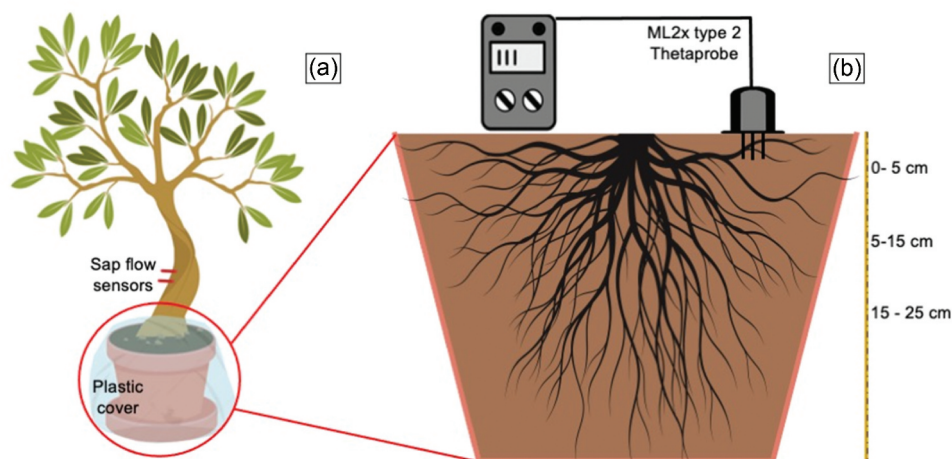


Figure 1. (a) Sap flow sensors were installed in the trunk of the olive tree (*Olea europaea*) and placed in a 70 L pot covered by a plastic film; (b) cross-section of the soil profile in the pot with the positions of the ThetaProbe shown on the soil surface and the three soil sampling depths (0–5, 5–15, and 15–25 cm) for isotope measurements.

USA) at the Faculty of Science and Technology, Free University of Bozen-Bolzano (Italy) (Penna *et al.* 2010). The memory effect of laser-based measurements was minimized following the procedure reported by Penna *et al.* (2012).

2.2 Simulation of isotope transport in the potted olive tree experiment

We used Hydrus-1D to simulate one-dimensional water flow and isotope transport in the potted olive tree system using the Richards and the advection-dispersion equations, respectively (Šimůnek *et al.* 2016).

The five van Genuchten parameters (θ_r , θ_s , α , n , and K_s) featured in the water retention and hydraulic conductivity functions were assessed through parameter optimisation (Supplementary material, Table S1). Irrigation supply and free drainage represent the upper and lower boundary conditions, respectively, whereas the potential evaporation (E_p) was assumed to be zero (see Section 2.1). Plant potential transpiration, T_p , determines the potential RWU that takes place within the soil profile. The maximum rooting depth was set to 42 cm, and root density was maximum at the soil surface and minimum at the soil profile bottom, based on the visual inspection at the end of the experiment (see Section 2.1). T_p was reduced by water stress to actual transpiration (T_a). The simulation period was set to 1234 hours. Hydraulic equilibrium was assumed as the initial condition by fixing $\psi = -42$ cm and $\psi = 0$ cm at the soil surface and soil profile bottom, respectively.

The observed isotopic composition of irrigation water was set as the concentration flux in the upper boundary condition, while a zero concentration gradient (free drainage) was set as the lower boundary condition. The initial isotope composition of -4 ‰ in $\delta^{18}\text{O}$ was set through the soil profile.

2.3 Determination of RWU source and transit time with the virtual tracer experiment

Another set of model simulations was carried out using the virtual tracer injection experiment to assess the temporal origin of RWU. The number of numerical simulations depended on the total number of irrigation events. There were 26 irrigation events, and therefore Hydrus-1D was run 26 times by assigning the i th $\delta^{18}\text{O}$ value to the i th irrigation event and then setting $\delta^{18}\text{O} = 0$ ‰ for all other irrigation events. The initial isotope composition across the soil profile was set to zero. RWU transit time, τ , is defined as the elapsed time between the irrigation inflow on the soil surface at time t_{in} and the RWU outflow of that water at time t_{out} (Sprengr *et al.* 2016).

We defined the tracer arrival time (t_{out}) as the cumulative root isotope uptake reaching 50% of the mass breakthrough curve (Sprengr *et al.* 2016). Therefore, τ was calculated as the difference between arrival time (t_{out}) and entry time (t_{in}) for each i th irrigation event. The relative irrigation contribution to actual transpiration was calculated as the ratio between isotope flux output (through actual RWU) and isotope flux input (through irrigation) (Sprengr *et al.* 2016).

3 Results

3.1 Simulation of isotope transport in the potted olive tree experiment

Figure 2 shows the soil water response to the irrigation. The successive irrigation events (blue bars in Fig. 2(a)) rapidly increased the soil water storage (wet conditions across the soil profile are indicated by the bluish colour in Fig. 2(b)), and the high transpiration rates induced a gradual desaturation of the soil profile after the irrigation events. These effects were enhanced near the soil surface (despite evaporation being largely absent), where root distribution was at its maximum.

Figure 3 shows that the soil isotopic composition reflected the water mixtures originating from all irrigation events. The vertical distribution of the $\delta^{18}\text{O}$ composition was quite uniform (bluish colour of soil water in Fig. 3(b)) when the irrigation events with local tap water ($\delta^{18}\text{O} = -7.97$ ‰, blue bars in Fig. 3(a)) were applied during the first (two-week) conditioning period. $\delta^{18}\text{O}$ values gradually decreased towards more depleted compositions when the irrigation events with labelled water ($\delta^{18}\text{O} = -12.75$ ‰, yellow bars in Fig. 3(a)) were applied during the second (five-week) period.

3.2 Determination of RWU source and transit time through the virtual tracer experiment

An illustrative example of the steps for assessing the transit time for two 3 L labelled irrigation events is shown in Fig. 4. The first event with tap water and the 14th event with labelled water are indicated by the black bars in Fig. 4(a) and (b). Isotope transport across the soil profile (Fig. 4(c) and (d)) depended on the frequency and amounts of irrigation events, actual transpiration, and drainage fluxes following the selected

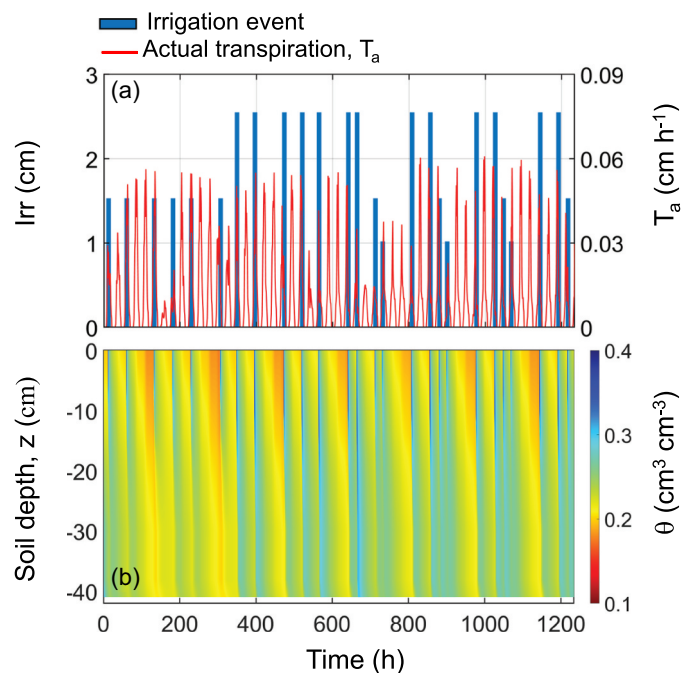


Figure 2. Hourly data of (a) water irrigation (Irr) events (blue bars) and actual transpiration, T_a (red line); and (b) soil water content, θ across the soil profile simulated in Hydrus-1D.

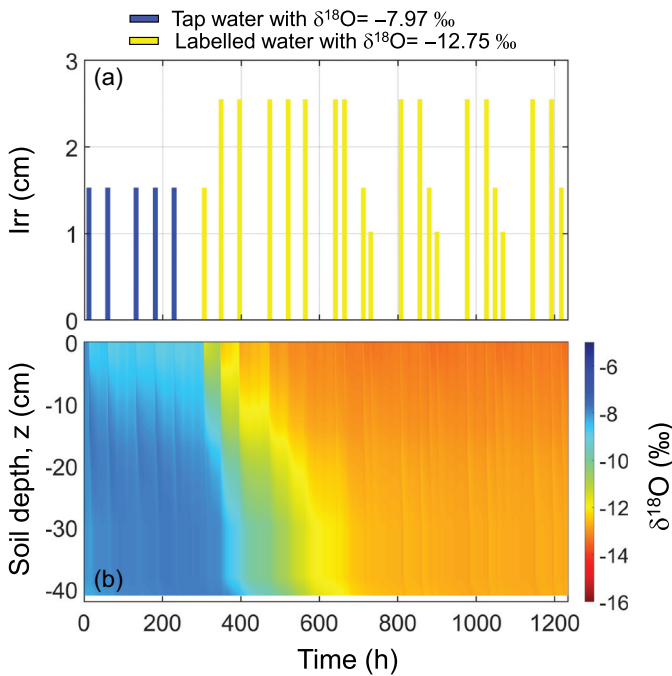


Figure 3. Hourly data of (a) tap water (blue bars with $\delta^{18}\text{O} = -7.97\text{‰}$) and labelled water (yellow bars with $\delta^{18}\text{O} = -12.75\text{‰}$); (b) $\delta^{18}\text{O}$ across the soil profile simulated in Hydrus-1D.

labelled irrigation event (Fig. 4(a) and (b)). The two events were characterized by very similar transit times ($\tau = 119\text{ h}$ and $\tau = 116\text{ h}$) even though the amount of transpired water in the first case (1st event) almost doubled the one in the second case (14th event). The proportion of *i*th irrigation isotope and cumulative root isotope uptake was 38.3% and 22.6% for the 1st and 14th irrigation events, respectively.

The descriptive statistics of RWU transit time and proportion of irrigation to actual transpiration are listed in Table 1, while all events are reported in Table A1 (Appendix). The first five irrigation events were characterized by tap water ($\delta^{18}\text{O} = -7.97\text{‰}$) in the conditioning period, while the remaining 21 events based on labelled water ($\delta^{18}\text{O} = -12.75\text{‰}$) were applied in the second, five-week-long period. It must be noted that the last five irrigation events were removed from data analysis because the arrival time occurred beyond the end of the model simulation.

The arrival time (t_{out}) and transit time (τ) values depended on water and isotope mass balance. As the labelled irrigation water moved through the soil profile, it carried its isotope concentration load as described by the advection-dispersion equation – meaning part of it was absorbed by roots (Fig. 4(e) and (f)), another part was lost by drainage at the base of the soil profile, and the remaining portion was retained in the soil (Fig. 4(c) and (d)). The mean irrigation supply and relative contributions of irrigation to actual transpiration were on average about 2.0 cm and 26%, respectively, allowing for the fact that evaporation was set to be zero while the remaining portion of irrigation water was lost by drainage. In other words, water in the amount of 0.52 cm was removed by roots under optimal water conditions with a mean transit time of about 95 h. The low coefficient of variation (below 30%) of τ and T_a/Irr

indicates the impact of regular irrigation management on water flow and isotope transport in the SPAC.

Figure 5 helps interpret RWU dynamics originating from each irrigation event. We note the similarity in shape between cumulative RWU (Fig. 5(a)) and root isotope uptake (Fig. 5(b)) patterns up until the arrival time. These curves represent the first half of RWU, as the arrival time was identified as when the cumulative root isotope uptake reached 50% of its final value. Ideally, the root isotope uptake sums would perfectly align with the corresponding RWU sums on a linear regression line (Fig. 5(c)). Instead, the data pairs scatter around the fitted linear regression line with a coefficient of determination (R^2) equal to 0.67, indicating that 67% of root isotope uptake variability is controlled by transpiration rates. Short transit times (bluish circles in Fig. 5(c)) are related to the steepest cumulative root isotope uptake curves (Fig. 5(b)).

4 Discussion

4.1 Quantifying irrigation uptake dynamics

Our proof-of-concept work used an ensemble simulation approach (the virtual tracer injection experiment) to trace soil water pathways in the SPAC originating from individual irrigation events. Any isotope concentration can be applied in the virtual tracer injection experiment, which enables the calculation of RWU transit time and the calculation of the contribution of irrigation water to plant transpiration. The repeated model simulations indicate that, on average, water travels across the soil for about 95 h (roughly corresponding to four days) before being taken up by roots. Moreover, the average irrigation depth is 2.02 cm, and about 26% of it is absorbed by the roots, according to the isotope mass balance. The water balance results show that the amount of water taken up by the roots was 14.1 cm, while the amount supplied by irrigation was 51.6 cm (RWU represents 27.3% of total irrigation). Therefore, the water balance approximates the isotope mass balance, in which RWU represents 25.6% of total irrigation.

The temporal origin of RWU from each irrigation event was determined by tracking root isotope uptake, which depended mainly on transpiration rates following the labelled irrigation event and on the isotope mass balance across the soil profile, which in turn was influenced by irrigation timing and amounts (Fig. 5). The regular irrigation management and transpiration fluxes induced low variability of transit time and irrigation partitioning values (Table 1).

In this study, the virtual tracer experiment combined the Richards equation and the advection-dispersion equations to simulate transit time in a potted olive tree experiment. This approach relies on the assumption that the arrival time corresponds to the time when the tracer mass breakthrough reaches 50% (Sprenger *et al.* 2016). Therefore, the virtual tracer experiment needs to be evaluated against other well-established approaches, such as the particle tracking algorithm or the water age equation. The former describes the advection-dominated flow pathways in the SPAC, while the latter explicitly models water age (e.g. Danesh-Yazdi *et al.* 2018, Zarlenga and Fiori 2020). However, such approaches

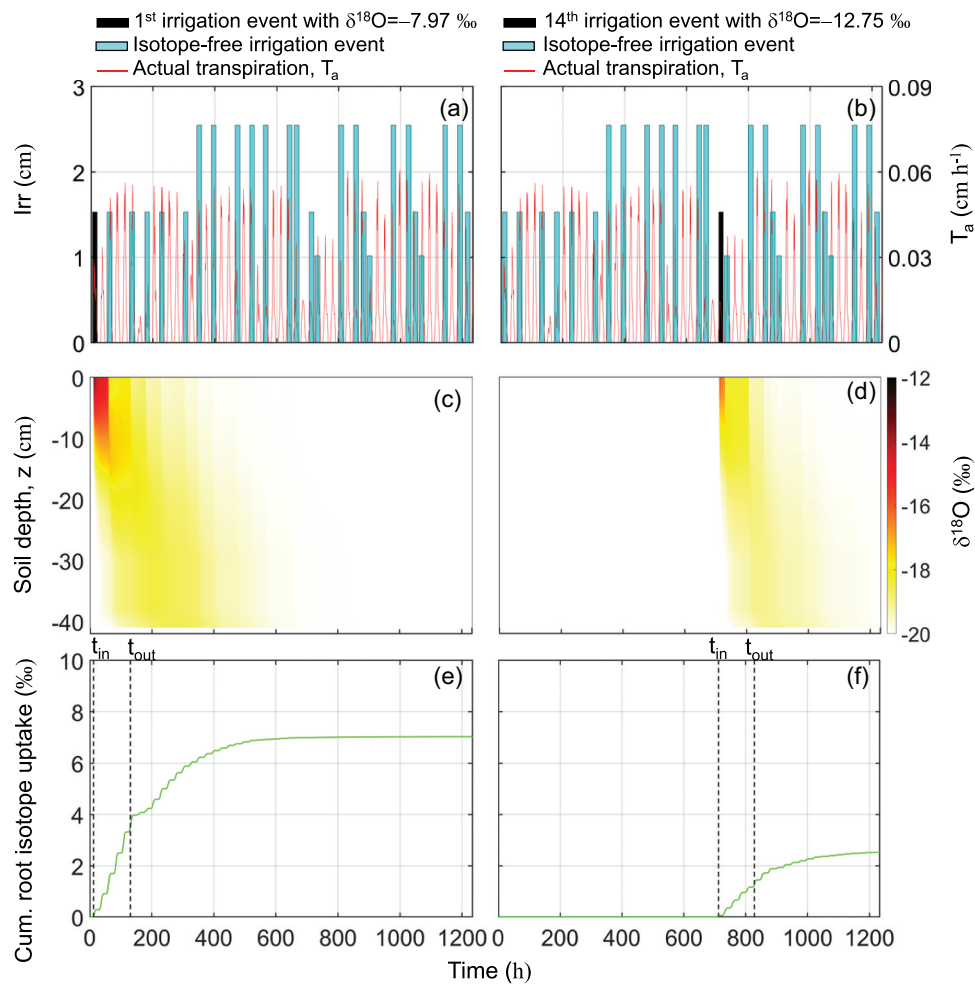


Figure 4. Hourly data of (a, b) tap water (1st event) and labelled water (14th event) irrigation (Irr) events (black bar) with known $\delta^{18}\text{O}$ signature, isotope-free irrigation events (cyan bars), and actual transpiration, T_a (red line); (c, d) $\delta^{18}\text{O}$ across the soil profile; (e, f) cumulative root $\delta^{18}\text{O}$ uptake (green line). Vertical dashed lines indicate entry (t_{in}) and arrival (t_{out}) times.

Table 1. Mean, standard deviation, coefficient of variation, minimum and maximum amounts of irrigation (Irr), transit time (τ), and irrigation contribution to actual transpiration (T_a/Irr) for the first 21 irrigation events used in this study. The last five events were ignored because their arrival time exceeded the time of the model simulation.

	Irr (cm)	τ (h)	T_a/Irr (%)
Mean	2.02	95.43	25.65
Standard deviation	0.59	22.24	7.53
Coefficient of variation	29.37	23.30	29.35
Min.	1.02	62.00	14.92
Max.	2.55	136.00	40.68

were tested mainly at catchment and hillslope scales (Wilusz *et al.* 2020, Zarlenga *et al.* 2022). A comparison between the virtual tracer experiment and other well-known approaches can be tested at the plot or tree scale, by exploiting hydrochemical measurements in isotope-labelled water experiments.

By raising model complexity (i.e. preferential flow in a heterogeneous soil profile, capillary rise from the shallow aquifer) in real-world situations, the temporal origin can reveal interesting aspects of the SPAC response to irrigation management and climate seasonality if well supported by *ad hoc*

measurements (Yin *et al.* 2015). Multi-modal transit time distributions are expected under seasonal climate regimes in field-scale applications.

4.2 Model limitations

Measurements of soil water content and $\delta^{18}\text{O}$ at different soil depths were integrated to optimize the soil hydraulic properties in Hydrus-1D via inverse modelling (Groh *et al.* 2018, Zhou *et al.* 2022). This is presented in the Supplementary material (Fig. S1). We recognize that model oversimplification might increase the discrepancy between observed and simulated isotopic compositions at different soil depths. The RWU is controlled by the root depth, the root distribution, and the RWU water stress function (Feddes *et al.* 1978). In this study, we had the opportunity to visualize root depth and distribution with a destructive approach at the end of the experiment (see Amin *et al.* 2021), but the Feddes function merits particular attention for determining actual transpiration (Rabbel *et al.* 2018, de Melo and de Jong van Lier 2021). Model simulations were validated using independent observations of sap flow and isotope composition in xylem water (Supplementary material, Fig. S2). In our analysis, we assumed that no fractionation occurred in either evaporation

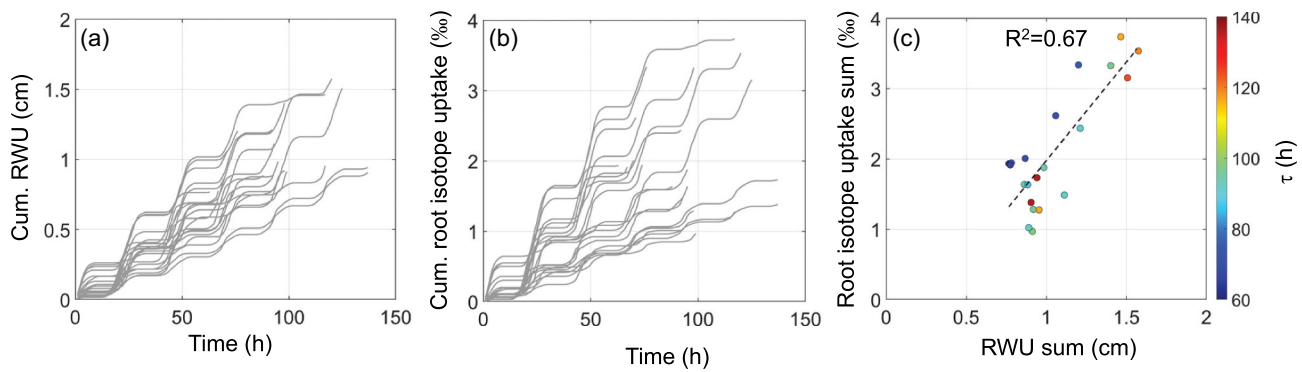


Figure 5. (a) Cumulative root water uptake (RWU) until arrival time for each irrigation event; (b) cumulative root isotope uptake until arrival time for each irrigation event; (c) relationship between RWU and root isotope uptake sums with dashed line indicating the fitting linear regression equation with corresponding coefficient of determination (R^2). The circles are colour-coded according to the corresponding RWU transit time (τ).

from the soil surface (along the pathway from the soil up to the roots) or transpiration (along the pathway from the roots up to the leaves). This assumption was verified for this specific case study (Amin *et al.* 2021), but is not generally applicable to other locations and other climate conditions (Martín-Gómez *et al.* 2016, Poca *et al.* 2019, de Deurwaerder *et al.* 2020).

5 Concluding remarks

The use of a combined isotope tracing and Hydrus-1D approach was able to quantify the temporal origin of water taken up by roots in a potted olive tree. The water parcels introduced with irrigation events were virtually traced across the soil profile to assess RWU transit time and the proportion of irrigation water to actual transpiration. The statistical distribution of transit times represents a functional indicator that can be used to characterize the reaction of the SPAC to irrigation management and climate seasonality. The results presented in this study pave the way for future field applications in which long-term model simulations will generate site-specific transit time distributions of all water balance components (RWU, evaporation, and drainage) in response to adverse climate disturbances (i.e. drought).

Disclosure statement

No potential conflict of interest was reported by the authors.

Funding

This study was supported by the MiUR-PRIN Project “WATER mixing in the critical ZONE: observations and predictions under environmental changes – WATZON” [grant 2017SL7ABC]. The work described in this paper and related research have been conducted with the support of the Italian inter-University PhD course in Sustainable Development and Climate Change.

ORCID

Paolo Nasta <http://orcid.org/0000-0001-9654-566X>
 Giulia Zuecco <http://orcid.org/0000-0002-2125-0717>
 Chiara Marchina <http://orcid.org/0000-0002-8496-635X>
 Daniele Penna <http://orcid.org/0000-0001-6915-0697>
 Jeffrey J. McDonnell <http://orcid.org/0000-0002-3880-3162>

Anam Amin <http://orcid.org/0000-0003-3202-8246>
 Marco Borga <http://orcid.org/0000-0003-3435-2779>
 Nunzio Romano <http://orcid.org/0000-0001-7276-6994>

References

- Aguzzoni, A., *et al.*, 2022. Water uptake dynamics in apple trees assessed by an isotope labeling approach. *Agricultural Water Management*, 266, 107572. doi:10.1016/j.agwat.2022.107572
- Allen, R., *et al.*, 1998. Crop evapotranspiration. FAO Irrigation and drainage paper 56. *Irrigation and Drainage*, 300 (56), 326.
- Amin, A., *et al.*, 2021. No evidence of isotopic fractionation in olive trees (*Olea europaea*): a stable isotope tracing experiment. *Hydrological Sciences Journal*, 66 (16), 2415–2430. doi:10.1080/02626667.2021.1987440
- Asadollahi, M., *et al.*, 2022. Toward a closure of catchment mass balance: insight on the missing link from a vegetated lysimeter. *Water Resources Research*, 58, e2021WR030698. doi:10.1029/2021WR030698
- Barbeta, A., *et al.*, 2022. Evidence for distinct isotopic composition of sap and tissue water in tree stems: consequences for plant water source identification. *New Phytologist*, 233, 1121–1132. doi:10.1111/nph.17857
- Benettin, P., *et al.*, 2021. Tracing and closing the water balance in a vegetated lysimeter. *Water Resources Research*, 57, e2020WR029049. doi:10.1029/2020WR029049
- Beyer, M., *et al.*, 2018. Examination of deep root water uptake using anomalies of soil water stable isotopes, depth-controlled isotopic labeling and mixing models. *Journal of Hydrology*, 566, 122–136. doi:10.1016/j.jhydrol.2018.08.060
- Beyer, M. and Penna, D., 2021. On the spatio-temporal under-representation of isotopic data in ecohydrological studies. *Frontiers in Water*, 3, 643013. doi:10.3389/frwa.2021.643013
- Brunetti, G., *et al.*, 2020. Handling model complexity with parsimony: numerical analysis of the nitrogen turnover in a controlled aquifer model setup. *Journal of Hydrology*, 584, 124681. doi:10.1016/j.jhydrol.2020.124681
- Chen, G., *et al.*, 2022. Soil water transport and plant water use patterns in subsidence fracture zone due to coal mining using isotopic labeling. *Environmental Earth Sciences*, 81 (310). doi:10.1007/s12665-022-10421-w
- Danesh-Yazdi, M., *et al.*, 2018. Bridging the gap between numerical solutions of travel time distributions and analytical storage selection functions. *Hydrological Processes*, 32, 1063–1076. doi:10.1002/hyp.11481
- de Deurwaerder, H.P.T., *et al.*, 2020. Causes and consequences of pronounced variation in the isotope composition of plant xylem water. *Biogeosciences*, 17 (19), 4853–4870. doi:10.5194/bg-17-4853-2020
- de Melo, M.L.A. and de Jong van Lies, Q., 2021. Revisiting the Feddes reduction function for modelling root water uptake and crop

- transpiration. *Journal of Hydrology*, 603, 126952. doi:10.1016/j.jhydrol.2021.126952
- Feddes, R.A., Kowalik, P.J., and Zaradny, H., 1978. *Simulation of Field Water Use and Crop Yield*. New York, NY: John Wiley & Sons.
- Gelhar, L.W., Welty, C., and Rehfeldt, K.R., 1992. A critical review of data on field-scale dispersion in aquifers. *Water Resources Research*, 28, 1955–1974. doi:10.1029/92WR00607
- Granier, A., 1985. Une nouvelle methode pour la mesure du flux de seve brute dans le tronc des arbres. *Annales des Sciences Forestières*, 42 (2), 193–200. doi:10.1051/forest:19850204
- Groh, J., et al., 2018. Inverse estimation of soil hydraulic and transport parameters of layered soils from water stable isotope and lysimeter data. *Vadose Zone Journal*, 17, 170168. doi:10.2136/vzj2017.09.0168
- Jackisch, C., et al., 2020. Estimates of tree root water uptake from soil moisture profile dynamics. *Biogeosciences*, 17, 5787–5808. doi:10.5194/bg-17-5787-2020
- Kahmen, A., et al., 2021. Dynamic ^2H irrigation pulse labelling reveals rapid infiltration and mixing of precipitation in the soil and species-specific water uptake depths of trees in a temperate forest. *Ecohydrology*, 14 (6), e2322. doi:10.1002/eco.2322
- Koeniger, P., et al., 2011. An inexpensive, fast, and reliable method for vacuum extraction of soil and plant water for stable isotope analyses by mass spectrometry. *Rapid Communications in Mass Spectrometry*, 25 (20), 3041–3048. doi:10.1002/rcm.5198
- Martin-Gómez, P., et al., 2016. Short-term dynamics of evaporative enrichment of xylem water in woody stems: implications for ecohydrology. *Tree Physiology*, 37, 511–522. doi:10.1093/treephys/tpw115
- Mennekes, D., et al., 2021. Ecohydrological travel times derived from in situ stable water isotope measurements in trees during a semi-controlled pot experiment. *Hydrology and Earth System Sciences*, 25, 4513–4530. doi:10.5194/hess-25-4513-2021
- Nasta, P., et al., 2021. Assessing the nitrate vulnerability of shallow aquifers under Mediterranean climate conditions. *Agricultural Water Management*, 258, 107208. doi:10.1016/j.agwat.2021.107208
- Penna, D., et al., 2010. On the reproducibility and repeatability of laser absorption spectroscopy measurements for $\delta^2\text{H}$ and $\delta^{18}\text{O}$ isotopic analysis. *Hydrology and Earth System Sciences*, 14, 1551–1566. doi:10.5194/hess-14-1551-2010
- Penna, D., et al., 2012. Technical note: evaluation of between-sample memory effects in the analysis of $\delta^2\text{H}$ and $\delta^{18}\text{O}$ of water samples measured by laser spectroscopes. *Hydrology and Earth System Sciences*, 16, 3925–3933. doi:10.5194/hess-16-3925-2012
- Penna, D., et al., 2018. Ideas and perspectives: tracing ecosystem water fluxes using hydrogen and oxygen stable isotopes—Challenges and opportunities from an interdisciplinary perspective. *Biogeosciences*, 15 (21), 6399–6415. doi:10.5194/bg-15-6399-2018
- Penna, D., et al., 2020. Water sources for root water uptake: using stable isotopes of hydrogen and oxygen as a research tool in agricultural and agroforestry systems. *Agriculture, Ecosystems & Environment*, 291, 106790. doi:10.1016/j.agee.2019.106790
- Penna, D., et al., 2021. Water uptake of apple trees in the Alps: where does irrigation water go? *Ecohydrology*, 14. doi:10.1002/eco.2306
- Poca, M., et al., 2019. Isotope fractionation during root water uptake by *Acacia caven* is enhanced by arbuscular mycorrhizas. *Plant and Soil*, 441, 485–497. doi:10.1007/s11104-019-04139-1
- Rabbet, I., et al., 2018. Using sap flow data to parameterize the feddes water stress model for norway spruce. *Water*, 10, 279. doi:10.3390/w10030279
- Rallo, G., et al., 2010. Agro-hydrological models to schedule irrigation of Mediterranean tree crops. *Italian Journal of Agrometeorology*, 1, 11–21.
- Romano, N., 1993. Use of an inverse method and geostatistics to estimate soil hydraulic conductivity for spatial variability analysis. *Geoderma*, 60, 169–186. doi:10.1016/0016-7061(93)90025-G
- Romano, N. and Santini, A., 1999. Determining soil hydraulic functions from evaporation experiments by a parameter estimation approach: experimental verifications and numerical studies. *Water Resources Research*, 35, 3343–3359. doi:10.1029/1999WR900155
- Schaap, M.G. and Leij, F.J., 2000. Improved prediction of unsaturated hydraulic conductivity with the Mualem-van Genuchten model. *Soil Science Society of America Journal*, 64, 843–851. doi:10.2136/sssaj2000.643843x
- Schelle, H., et al., 2012. Inverse estimation of soil hydraulic and root distribution parameters from lysimeter data. *Vadose Zone Journal*, 11 (4). doi:10.2136/vzj2011.0169
- Šimůnek, J., Šejna, M., and van Genuchten, M.T., 2016. Recent developments and applications of the HYDRUS computer software packages. *Vadose Zone Journal*, 15, 1–25. doi:10.2136/vzj2016.04.0033
- Sprenger, M., et al., 2015. Estimating flow and transport parameters in the unsaturated zone with pore water stable isotopes. *Hydrology and Earth System Sciences*, 19, 2617–2635. doi:10.5194/hess-19-2617-2015
- Sprenger, M., et al., 2016. Travel times in the vadose zone: variability in space and time. *Water Resources Research*, 52, 5727–5754. doi:10.1002/2015WR018077
- Stumpp, C., et al., 2012. Effects of land cover and fertilization method on water flow and solute transport in five lysimeters: a long-term study using stable water isotopes. *Vadose Zone Journal*, 11 (1). doi:10.2136/vzj2011.0075
- Vanderborght, J. and Vereecken, H., 2007. Review of dispersivities for transport modelling in soils. *Vadose Zone Journal*, 6, 29–52. doi:10.2136/vzj2006.0096
- van Genuchten, M.T., 1980. A closed form equation for predicting the hydraulic conductivity of unsaturated soils. *Soil Science Society of America Journal*, 44, 892–898. doi:10.2136/sssaj1980.03615995004400050002x
- von Freyberg, J., et al., 2020. Plant and root-zone water isotopes are difficult to measure, explain, and predict: some practical recommendations for determining plant water sources. *Methods in Ecology and Evolution*, 11 (11), 1352–1367. doi:10.1111/2041-210x.13461
- Wilusz, D.C., et al., 2020. Using particle tracking to understand flow paths, age distributions, and the paradoxical origins of the inverse storage effect in an experimental catchment. *Water Resources Research*, 56, e2019WR025140. doi:10.1029/2019WR025140
- Yin, L., et al., 2015. Interaction between groundwater and trees in an arid site: potential impacts of climate variation and groundwater abstraction on trees. *Journal of Hydrology*, 528, 435–448. doi:10.1016/j.jhydrol.2015.06.063
- Zarlenga, A. and Fiori, A., 2020. Physically based modelling of water age at the hillslope scale: the boussinesq age equations. *Hydrological Processes*, 34 (12), 2694–2706. doi:10.1002/hyp.13755
- Zarlenga, A., Fiori, A., and Cvetkovic, V., 2022. On the interplay between hillslope and drainage network flow dynamics in the catchment travel time distribution. *Hydrological Processes*, 36 (3), e14530. doi:10.1002/hyp.14530
- Zhou, T., et al., 2022. The impact of evaporation fractionation on the inverse estimation of soil hydraulic and isotope transport parameters. *Journal of Hydrology*, 612, 128100. doi:10.1016/j.jhydrol.2022.128100

Appendix

Table A1. Entry time (t_{in}), irrigation amount (Irr) and $\delta^{18}O$, arrival time (t_{out}), transit time (τ), and rainfall contribution to actual transpiration (T_a/Irr) for the 26 irrigation events used in this study. The last five events were ignored in the data analysis.

t_{in} (h)	Irr (cm)	$\delta^{18}O$ (‰)	t_{out} (h)	τ (h)	T_a/Irr (%)
12	1.53	-8.0	131	119	38.3
60	1.53	-8.0	176	116	40.7
132	1.53	-8.0	256	124	34.2
181	1.53	-8.0	278	97	36.5
229	1.53	-8.0	304	75	36.2
306	1.53	-12.7	398	92	26.7
349	2.55	-12.7	440	91	26.3
396	2.55	-12.7	466	70	28.3
473	2.55	-12.7	535	62	21.0
520	2.55	-12.7	614	94	17.3
564	2.55	-12.7	637	73	20.3
641	2.55	-12.7	777	136	14.9
664	2.55	-12.7	800	136	18.6
712	1.53	-12.7	828	116	22.6
731	1.02	-12.7	829	98	26.1
808	2.55	-12.7	877	69	21.7
856	2.55	-12.7	950	94	20.3
880	1.53	-12.7	977	97	22.9
900	1.02	-12.7	992	92	27.3
977	2.55	-12.7	1043	66	20.6
1026	2.55	-12.7	1113	87	17.7
1048	1.53	-12.7	1117	69	21.2
1068	1.02	-12.7	1118	50	24.7
1144	2.55	-12.7	1187	43	10.5
1192	2.55	-12.7	1212	20	4.0
1217	1.53	-12.7	1232	15	1.1